HACETTEPE JOURNAL OF BIOLOGY AND CHEMISTRY Research Article
Hacettepe J. Biol. & Chem., 2009, 37 (2) 157-168

Poly(hydroxyethyl methacrylate) Nanoparticles for Environmental Applications

Deniz Türkmen[1], Veyis Karakoç[1], Lokman Uzun[1], Nevra Öztürk[2], Sinan Akgöl[2] and Adil Denizli[1]

[1]Department of Chemistry, Hacettepe University, Ankara, Turkey

[2]Department of Chemistry, Adnan Menderes University, Aydın, Turkey

Article Info

Article history:

Received
February 12, 2009

Received in revised form
March 21, 2009

Accepted
March 24, 2009

Available online
June 28, 2009

Key Words

Nanoparticles;
Mercury Removal,
Environmental
remediation

Abstract

The poly(hydroxyethyl methacrylate) (PHEMA) nanoparticles with an average size of 150 nm in diameter and with a polydispersity index of 1.171 were produced by a surfactant free emulsion polymerization. Specific surface area of the PHEMA nanoparticles was found to be 1779 m^2/g. 3-(2-Imidazoline-1-yl)propyl(triethoxysilane) (IMEO) was covalently attached to the nanoparticles as a metal-complexing ligand. The PHEMA-IMEO nanoparticles were used for the removal of Hg^{2+} ions from synthetic solutions. To evaluate the degree of IMEO loading, the PHEMA nanoparticles were subjected to Si analysis by using flame atomizer atomic absorption spectrometer and it was estimated as 280 mg IMEO/g of polymer (1021 μmol/g). The PHEMA nanoparticles were characterized by atomic force microscopy (AFM), scanning electron microscopy (SEM) and fourier transform infrared spectroscopy (FTIR). Adsorption equilibrium was achieved in about 10 min. The adsorption amount of Hg^{2+} ions onto the PHEMA nanoparticles was negligible (0.14 mg/g). The IMEO attachment significantly increased the Hg^{2+} adsorption amount (746 mg/g). Adsorption amount of PHEMA-IMEO nanoparticles increased significantly with increasing Hg^{2+} concentration. The adsorption of Hg^{2+} ions increased with increasing pH and reached a plateau value at around pH 5.0. Competitive heavy metal adsorption from aqueous solutions containing Cd^{2+}, Pb^{2+} and Hg^{2+} was also investigated. The competitive adsorption capacities are 238.8 mg/g for Hg^{2+}; 45.9 mg/g for Cd^{2+} and 19.6 mg/g for Pb^{2+}. These results may be considered as an indication of higher specificity of the PHEMA-IMEO nanoparticles for the Hg^{2+} comparing to other ions. Consecutive adsorption and elution operations showed the feasibility of repeated use for PHEMA-IMEO nanoparticles.

INTRODUCTION

Nanotechnology is a enabling technology that deals with nano-meter sized objects [1]. It is expected that nanotechnology will be developed at several levels: materials, devices and systems. The nanomaterials level is the most advanced at present, both in scientific knowledge and in commercial applications. A decade ago, nanoparticles were studied because of their size-dependent physical and chemical properties [2]. Now they have entered a commercial exploration period [3]. Many published works focused on the synthesis of micrometer-sized polymer matrix [4]. Only limited work has been

* Correspondence to: Adil Denizli,

Hacettepe University, Department of Chemistry, Biochemistry Division, Beytepe, Ankara

Tel: +90312 297 7983 Fax: +90312 299 2163

E-mail: denizli@hacettepe.edu.tr

published on the application of nanosized particles in the adsorption of heavy metal ions. Nanosized particles can produce larger specific surface area and, therefore, may result in high binding capacity for metal ions. Therefore, it may be useful to synthesize nanosized particles and utilize them for the removal of heavy metal ions [5-10].

Surface modification can be accomplished by physical/chemical binding or surface coating of desired molecules, depending on the specific applications [11]. Surface modifications is an active research area in the fields of microelectronics, biotechnology and material science. The properties like adhesion, wettability, biocompatibility and binding affinity of the surface can be altered and tuned to the specific requirements by chemical or physical modification of the surfaces [12]. Modified materials are nowadays well-known and have been investigated intensively due to their potential applications in many areas, such as biology, medicine and environment. Surface modification of particles by organic compounds can be achieved via; organic vapour condensation, polymer coating, surfactant binding and direct silanization. Direct silanization is attractive for improving stability and control of surface properties [13].

Mercury is a common pollutant of water, resulting from the burning of coal by power plants, and in the inappropriate disposal from batteries, paints, lights, and industrial by products. Mercury poisoning is becoming more important because of the extensive contamination of water and fish and the increasing consumption of fish in the human diet [14]. Mercury is cytotoxic, exerting its effect by depleting the thiol reserves in the mitochondria, resulting in cell death. It is extremely neurotoxic, and leads to dizziness, irritability, tremor, depression, and memory loss [15]. It is also toxic to the kidneys and colon, the 2 main sites of excretion. Mercury is released very slowly from the body with a half-life of at least 60 days, resulting in increasing amounts with chronic consumption of contaminated fish [16].

In the gastrointestinal tract methylmercury (MeHg) is absorbed to approximately 95%, Hg^{2+} to approximately 7% and elemental Hg to less than 0.01%. The absorption of elemental mercury (Hg°) in the lung is about 80%. Within tissues, MeHg is slowly demethylated to Hg^{2+}. Elemental mercury is rapidly oxidized to the mercurous form (Hg^{+}) and then to the mercuric form (Hg^{2+}) in blood by catalase [17]. However, the time that this transformation takes is sufficient for Hg° to reach central nervous system, which is its primary target [18]. The kidney is considered the target organ for the mercurous and mercuric forms, but these forms are also known to accumulate readily in virtually all ectodermal and endodermal epithelial cells and glands. Once at the target tissues, the mercury entities exert a variety of cytotoxic effects, generally as a result of binding to sulfhydryl groups [19].

The goal of this paper is to report the synthesis of poly(hydroxyethyl methacrylate) [PHEMA] nano-particles carrying reactive imidazole [3-(2-imidazo-line-1-yl)propyl(triethoxysilane), IMEO] and on their use in the adsorptive removal of Hg^{2+} ions from synthetic solutions by metal-chelation. PHEMA nanoparticles (150 nm in diameter) were produced by a surfactant free emulsion polymeri-zation technique. Then, IMEO was attached to the nanoparticles as a metal complexing agent. The PHEMA-IMEO nanoparticles were characterized by AFM, SEM and FTIR. Removal studies were conducted to evaluate the binding capacity of Hg^{2+} onto the PHEMA-IMEO nanoparticles. Elution of Hg^{2+} and regeneration of the silanized nanoparticles were also tested.

MATERIALS AND METHODS

Chemicals

Hydroxyethyl methacrylate (HEMA, Sigma Chem. Co., St. Louis, USA) and ethylene glycol dimethacrylate (EGDMA, Aldrich, Munich, Germany) were distilled under vacuum (100 mmHg). 3-(2-Imidazoline-1-yl)propyl(triethoxysilane) (IMEO, molecular weight: 274.43 g/mol) was purchased from Sigma. Poly(vinyl alcohol) (molecular weight: 100 000, 98% hydrolyzed) was purchased from Aldrich (Munich, Germany). All other chemicals were of the highest purity commercially available and were used without further purification. All water used in the experiments was purified using a Barnstead (Dubuque, IA) ROpure LP® reverse osmosis unit with a high flow cellulose acetate membrane (Barnstead D2731) followed by a Barnstead D3804 NANOpure® organic/colloid removal and ion exchange packed bed system.

Synthesis of PHEMA nanoparticles

Surfactant free emulsion polymerization was carried out according to the literature procedure with minor modifications as reported elsewhere [20]. Briefly, the stabilizer, PVAL (0.5 g), was dissolved in 50 ml deionized water for the preparation of the continuous phase. Then, the monomer mixture 0.6 ml/0.01 ml (HEMA/EGDMA) was added to the dispersion which was mixing in an ultrasonic bath for about half an hour. Potassium persulphate (KPS, initiator) concentration in monomer phase was 0.44 mg/ml. Prior to polymerization, initiator was added to the solution and nitrogen gas blown through the medium for about 1–2 min to remove dissolved oxygen. Polymerization was carried out in a constant temperature shaking bath at 70°C, under nitrogen athmosphere for 24 h. After the polymerization, the nanoparticles were cleaned by washing with methanol and water several times to remove the unreacted monomers. For this purpose, the nanoparticles were precipitated and collected with the help of a centrifuge (Zentrifugen, Universal 32 R, Germany) which is the rate of 18 000 g for 1 h and resuspended in methanol and water several times. After that, the PHEMA nanoparticles were further washed with deionized water.

Silanization of PHEMA particles

Silane is a coupling agent and its bifunctional molecule bonds to both the exposed composite filler particles and the bonding resin [21]. The silane compounds readily react with the surface hydroxyl groups of the different supports [22]. It is assumed in the literature that the silane molecules are first hydrolyzed by the trace quantities of water present either on the surface of the support or in the solvent followed by the formation of a covalent bond with the surface [23]. For the silanization, PHEMA nanoparticles and IMEO (mol ratio 1:10) were mixed and stirred at 25°C for about 4 days. At the end of this period, stirring was stopped. The silanization reaction takes place at 25°C without any catalyst as shown in Figure 1. The resulting silanized

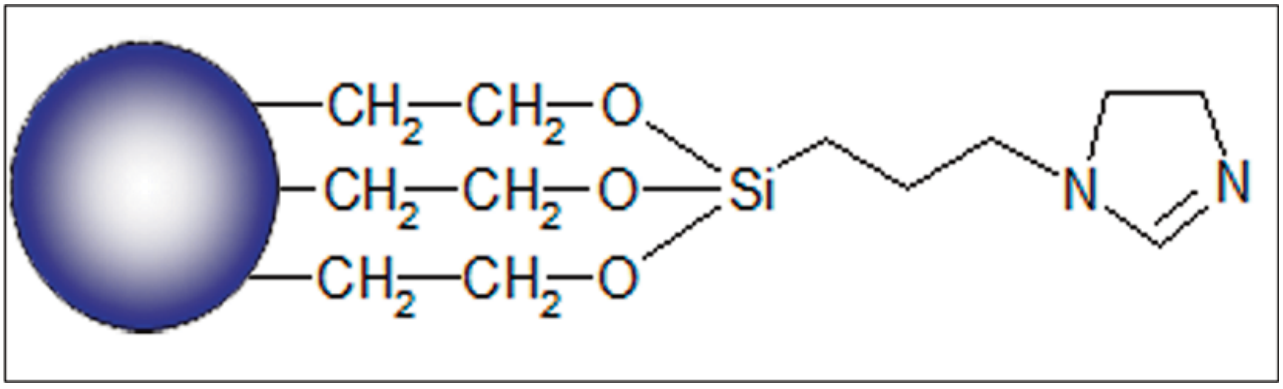

Figure 1. Structure of the PHEMA-IMEO nanoparticles.

nanoparticles were centrifuged and washed with dichloromethane. Then, the nanoparticles were resuspended in distilled water. To evaluate the degree of silanization (i.e., IMEO loading), the PHEMA nanoparticles were subjected to Si analysis using flame atomizer atomic absorption spectrometer (AAS, AAnalyst 800, Perkin Emler, USA). The structure of the PHEMA-IMEO nanoparticles is given in Figure 1.

Characterization Experiments

The average particle size and size distribution were determined by Zeta Sizer (Malvern Instruments, Model 3000 HSA, England).

The size distribution of the nanoparticles was examined by scanning electron microscopy (SEM, Philis, XL-30S FEG, Germany). The nanoparticle sample was initially dried in air at 25°C before being analyzed. The sample was mounted on a SEM sample mount and was sputter coated for 2 min. The sample was then mounted in a SEM. The sample was then scanned at the desired magnification.

The size of the PHEMA nanoparticles was also analyzed by atomic force microscopy (AFM) (Digital Instruments, MMafm-2/1700 EXL). Scanning was performed at a scan rate of 1.001 Hz and scan size of 5 μm. The tip loading force was minimized to avoid structural changes of the sample.

FTIR spectra of the IMEO, the PHEMA and the PHEMA-IMEO nanoparticles were obtained using a FTIR spectrophotometer (Varian FTS 7000, USA). The dry nanoparticles (about 0.1 g) were thoroughly mixed with KBr (0.1 g, IR Grade, Merck, Germany), and pressed into a tablet form and the spectrum was recorded. To prepare a liquid sample (e.g., IMEO) to FTIR analysis, firstly place a drop of the liquid on the face of a highly polished KBr (0.1 g, IR Grade, Merck, Germany) plate, then place a second plate on top of the first plate so as to spread the liquid in a thin layer between the plates, and clamps the plates together. Finally wipe off the liquid out of the edge of plate, and the spectrum was then recorded.

To evaluate the degree of silanization, the PHEMA nanoparticles were subjected to Si analysis using flame atomizer atomic absorption spectrometer (AAS).

The surface area of the PHEMA nanoparticles was calculated using the following expression:

$$N = 6.10^{10}. S / \pi.\rho s.d^3 \quad (1)$$

Here, N is the number of nanoparticles per milliliter; S is the % of solids; ρs is the density of bulk polymer (g/mL); d is the nanoparticle diameter (nm). The number of nanoparticles in mL suspension was determined by utilizing from mass-volume graph of nanoparticles. From all these data, specific surface area of the PHEMA nanoparticles were calculated by multiplying N and surface area of 1 nanoparticle.

Hg^{2+} Adsorption Studies

Adsorption of Hg^{2+} from aqueous solutions was investigated in batch experiments. Effects of Hg^{2+} concentration and pH of the medium on the adsorption rate and capacity were studied. 100 mL aliquots of aqueous solutions containing different amounts of Hg^{2+} (in the range of 10-500 mg/L) were treated with the nanoparticles at different pH (in the range of 2.0-7.0) (adjusted with HCl-NaOH). The nanoparticles (100 mg) were stirred with a mercury nitrate salt solution at room temperature for 2 h. All glassware for adsorption experiments was washed with 1.0 M HNO_3 and rinsed thoroughly with deionized water. The concentration of the Hg^{2+} in the aqueous phase was measured by using an Atomic Absorption Spectrophotometer. A Shimadzu Model AA-6800 Flame Atomic Absorption Spectrophotometer (Japan) was used. For Hg^{2+} determinations,

MVU-1A (Mercury Vapor Unit) was employed. Deuterium background correction was applied throughout the experiments and the spectral slit width was 0.5 nm. The instrument response was periodically checked with a known Hg^{2+} solution standard. The adsorption experiments were performed in replicates of three and the samples were analyzed in replicates of three as well. For each set of data present, standard statistical methods were used to determine the mean values and standard deviations. Confidence intervals of 95% were calculated for each set of samples in order to determine the margin of error. The adsorption amount of the nanoparticles was calculated according to the mass balance on Hg^{2+} ion.

Competitive Adsorption

Competitive heavy metal adsorption from aqueous solutions containing Hg^{2+}, Cd^{2+} and Pb^{2+} was also investigated in a batch experimental system. A solution (100 ml) containing 10 mg/L of each metal ions was treated with the nanoparticles (100 mg) at a pH of 5.0, in the flasks stirred magnetically at 100 rpm. The temperature was maintained at 25°C. After a sufficient amount of time for equilibration, the solution was centrifuged, and the supernatant was removed and analyzed for remaining metal ions. The amounts of adsorbed heavy metal ions were then determined by difference. Equilibration time was relatively short; the adsorption experiment was completed in 30 h.

Desorption and Repeated Use

Desorption of Hg^{2+} ions was studied with 0.5% thiourea in 0.05 M HCl solution. The nanoparticles were placed in this desorption medium and stirred continuously (at a stirring rate of 600 rpm) for 15 min at room temperature. The desorption ratio was calculated from the amount of Hg^{2+} ions adsorbed on the nanoparticles and the final Hg^{2+} concentration in the desorption medium. In order to test the reusability of the nanoparticles, Hg^{2+} ions adsorption-desorption procedure was repeated twenty times using the same nanoparticles. In order to regenerate after desorption, the nanoparticles were washed with 0.1 M HNO_3.

RESULTS AND DISCUSSION

Nanoparticles can produce larger specific surface area and therefore may result in high metal-complexing ligand loading. Therefore, it may be useful to synthesize nanoparticles with large surface area and utilize them as suitable carriers for the

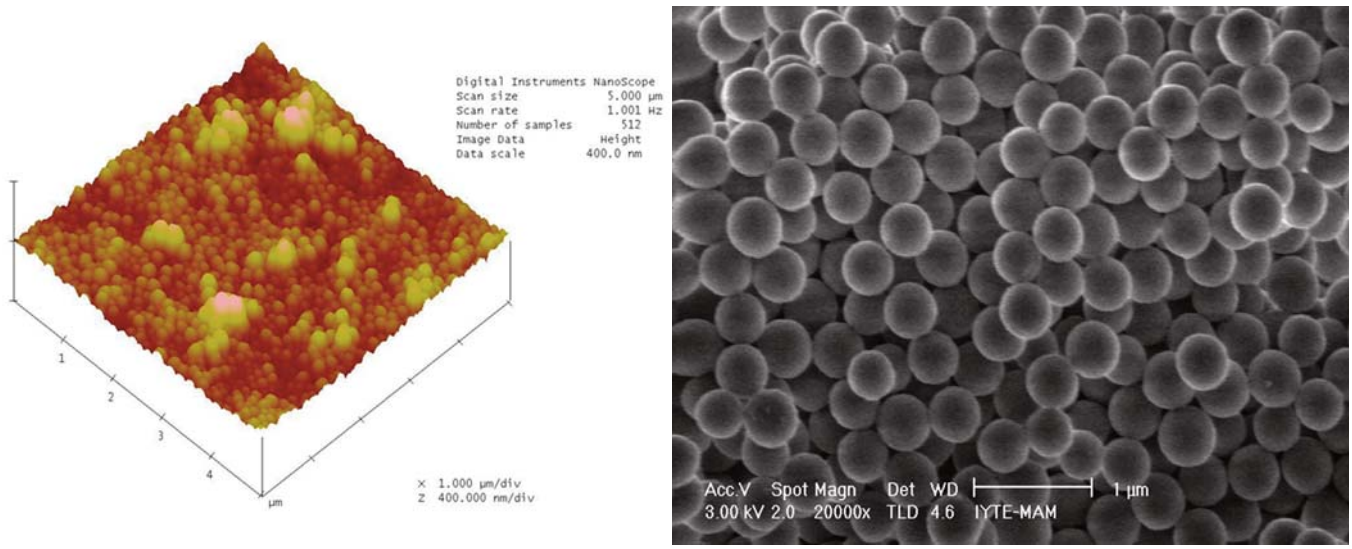

Figure 2. AFM and SEM images of PHEMA nanoparticles.

adsorption of metal ions. The spesific surface area was calculated as 1779 m^2/g. PHEMA nanoparticles with an average size of 150 nm in diameter and with a polydispersity index of 1.171 were produced by surfactant free emulsion polymerization. It is apparent that the PHEMA nanoparticles are perfectly spherical with a relatively smooth surface and uniform as shown by the atomic force microscopy (AFM) and scanning electron microscopy (SEM) images (Figure 2). The small polydispersity index suggest that nucleation is fast compared to particle growth, and also the absence of a secondary nucleation step. In addition, the total monomer conversion was determined as 98.5% (w/w) for PHEMA nanoparticles. PHEMA nanoparticles were highly dispersive in water by ultrasonication due to -OH groups on the surface of nanoparticles. The dispersion state of the particles was confirmed visually by the observed white color of the suspension. The aqueous dispersion phase of nanoparticles were stable for several days.

FTIR spectra of the IMEO, the PHEMA and the PHEMA-IMEO are shown in Figure 3. In the FTIR spectrum of the IMEO, the strong absorption bands at 1605 cm^{-1}, assigned to the characteristic ν(C=N) vibrations and indicated a strong band at 2928 and 2974 cm^{-1} ν(C-H) (Figure 3A). The ν(O-H) stretching vibration in PHEMA is observed in the 3600-3410 cm^{-1} range as broad absorptions, indicated a strong band at 1730 cm^{-1} due to ν(C=O) group and the 2954 cm^{-1} ν(C-H) stretching of CH_3, the 1268 cm^{-1}

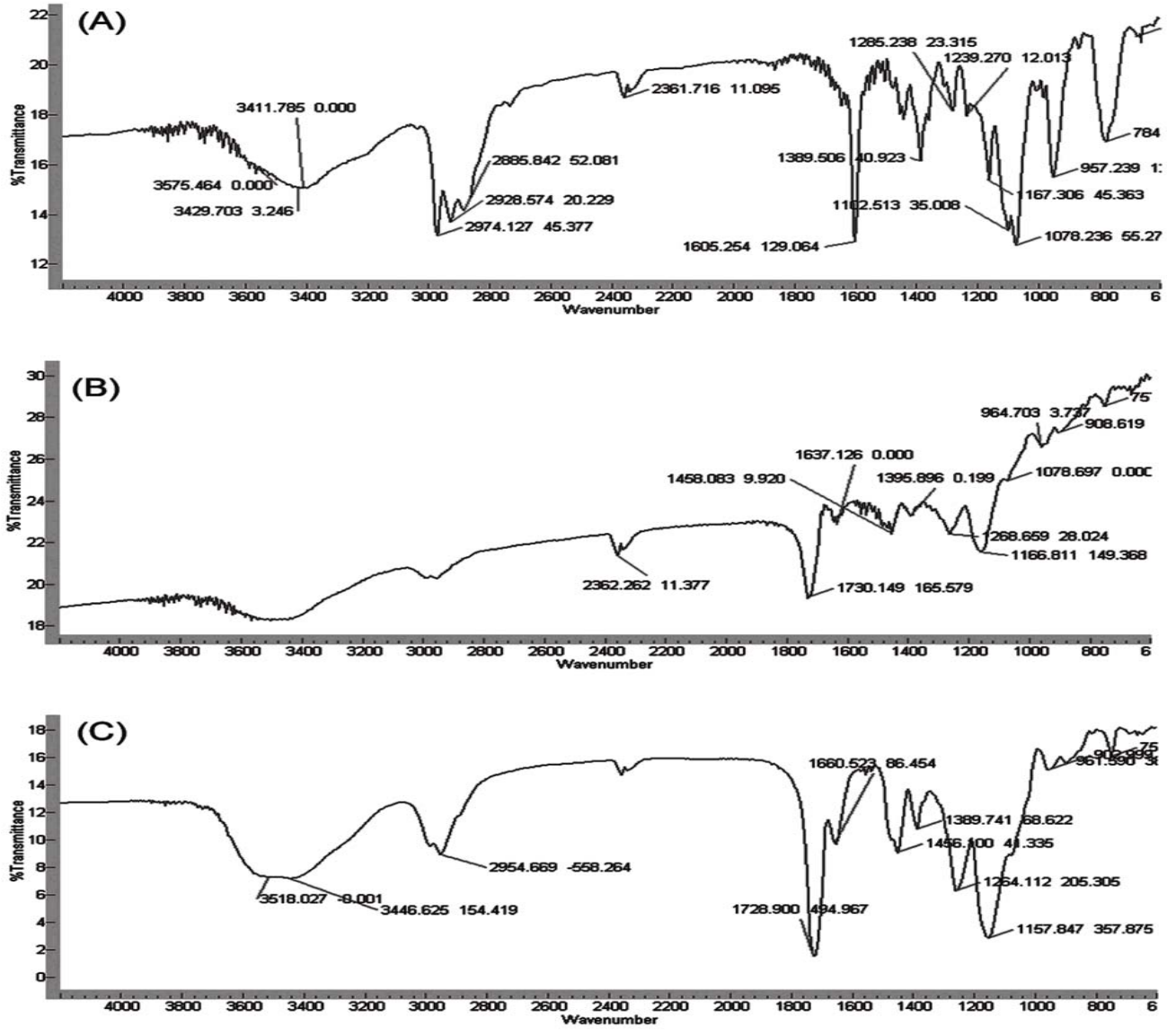

Figure 3. FTIR spectra of (A) IMEO; (B) PHEMA; (C) PHEMA-IMEO.

ν(C-O) stretching vibration (Figure 3B). The characteristic ν(C=O), ν(C=N) and ν(C-H) stretching vibration bands of the PHEMA-IMEO are observed at, 1728 cm^{-1}, 1660 cm^{-1}, 2954 cm^{-1} respectively (Figure 3C). In addition to, the n(Si-O-C) vibration band is observed in the 1264 cm^{-1}. As a result, the peak position of 1264 cm^{-1} is related to ν(Si-O-C) and the observance of C=N bands of the PHEMA-IMEO at 1660 cm^{-1}, the shifts of the C=N vibration to higher frequencies of 1660 cm^{-1} is due to the silanization of nanoparticles.

Effect of Hg^{2+} concentration

Figure 4 shows the equilibrium concentration of Hg^{2+} dependence of the adsorbed amount of the Hg^{2+} onto both the PHEMA and the PHEMA-IMEO nanoparticles. Adsorption of Hg^{2+} onto the PHEMA nanoparticles was very low, about 0.14 mg/g.

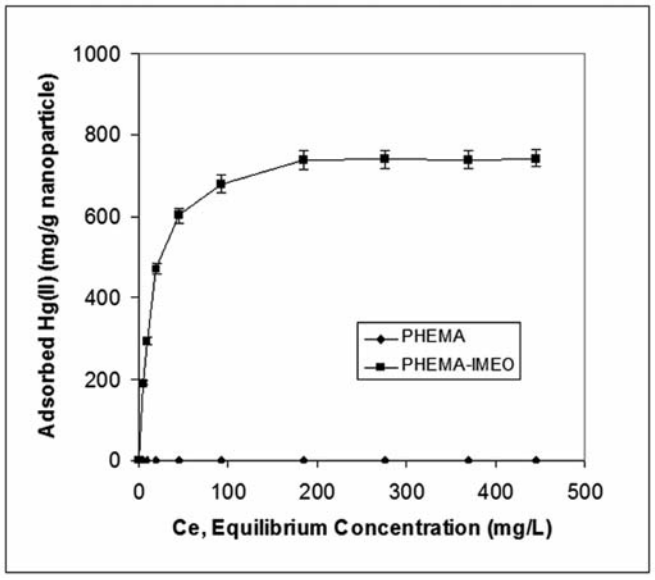

Figure 4. Effect of Hg^{2+} concentration on adsorption of Hg^{2+} on the PHEMA and PHEMA-IMEO nanoparticles; IMEO loading: 1021 μmol/g; pH: 5.0.

Because, PHEMA nanoparticles do not contain any binding sites for complexation of Hg^{2+}. This very low adsorption value of Hg^{2+} may be due to weak interactions between Hg^{2+} and hydroxyl groups on the surface of the PHEMA nanoparticles. However, IMEO incorporation into the polymer structure significantly increased the adsorption capacity to 746 mg/g. The adsorption values increased with increasing equilibrium concentration of Hg^{2+}, and a saturation value is achieved at ion concentration of 180 mg/L, which represents saturation of the active binding sites on the PHEMA-IMEO nanoparticles.

Different polymeric adsorbents carrying metal-chelating ligands with a wide range of adsorption capacities for Hg^{2+} ions have been reported (Table 1). Comparing the maximum adsorption capacities, it seems that the adsorption capacity achieved with the novel IMEO-attached PHEMA nanoparticles are rather satisfactory.

Adsorption Isotherms

Two important physico-chemical aspects for evaluation of the adsorption process as a unit operation are the kinetics and the equilibria of adsorption. Modelling of the equilibrium data has been done using the Langmuir, Freundlich and Langmuir-Freundlich isotherms [24]. The equations are represented as follows, respectively.

$$1/q_e = (1/q_{max}) + [1/(q_{max}\, b)]\ (1/C_e) \quad (2)$$

$$\log q_e = 1/n\ (\log C_e) + \log K_F \quad (3)$$

$$1/q_e = (1/q_{max}) + [1/(q_{max}\, b)]\ (1/C_e)^{1/n} \quad (4)$$

where, b is the Langmuir isotherm constant, K_F is the Freundlich constant, and n is the Freundlich exponent. 1/n is a measure of the surface heterogeneity ranging between 0 and 1, becoming more heterogeneous as its value gets closer to zero. q_{max} gives theoretical maximum adsorption capacity. The ratio of q_e gives the theoretical monolayer saturation capacity of nanoparticles.

Some model parameters were determined by nonlinear regression with commercially available software and are shown in Table 2. Comparison of

Table 1. Comparison of adsorption capacities of different adsorbents.

Adsorbent	Chelating Ligand	Capacity	REF
Styrene-divinylbenzene	Thiol	20 mg/g	[25]
PMMA	Ethylenediamine	30 mg/g	[26]
Polystyrene	Dithiocarbamate	32 mg/g	[27]
Poly(GMA-DVB)	Phosphoric acid	40 mg/g	[28]
PHEMA	Dithizone	42 mg/g	[29]
Polystyrene	Sulfur-chlorinated jajoba wax	50 mg/g	[30]
PEGDMA	Acrylamide	54 mg/g	[31]
Soy protein hydrogel	Ethylenediamine tetraacetic acid	60 mg/g	[32]
Magnetic poly(vinyl alcohol)	Procion Blue MX-3G	69 mg/g	[33]
N-Hydroxymethyl thioamide	Thioamide	72 mg/g	[34]
Poly(vinyl pyridine)	Dithizone	144 mg/g	[35]
Silica	3-trimethoxysilyl-1-propanethiol	184 mg/g	[36]
Silica Gel	Poly(ethyleneimine)	200 mg/g	[37]
Poly(N-vinylimidazole)	Imidazole	200 mg/g	[38]
PHEMA	Thiazolidine	222 mg/g	[39]
Cellulose	Poly(ethyleneimine)	288 mg/g	[40]
PHEMA	Poly(ethyleneimine)	334 mg/g	[41]
Amberlite IRC 718	Iminodiacetic acid	360 mg/g	[42]
PHEMA	N-Methacryloylcysteine	1018 mg/g	[43]
PHEMA	N-Methacryloylhistidine	1234 mg/g	[44]
Composite	Dithiocarbamate	157.3 mg/g	[45]
Poly(HEMA-MALA)	N-methacryloylalanine	168 mg/g	[46]
Magnetic Yeast	Yeast	114.6 mg/g	[47]
PHEMA	Polyethyleneimine	335 mg/g	[48]
Poly(HEMA-VIM)	Vinyl imidazole	163.5 mg/g	[49]
PHEMA	N-methacryloylglutamic acid	410 mg/g	[50]
PHEMA	IMEO	746 mg/g	in this study

Table 2. Adsorption parameters obtained from Langmuir, Freundlich and Langmuir-Freundlich isotherms.

	Langmuir			Freundlich			Langmuir-Freundlich			
q_{exp}, mg/g	q_{max}, mg/g	b, mL/mg	R^2	K_F	1/n	R^2	q_{max}, mg/g	b, mL/mg	1/n	R^2
743.0	769.2	0.0797	0.9930	170.0	0.2703	0.8728	1428.6	0.2333	0.2703	0.9132

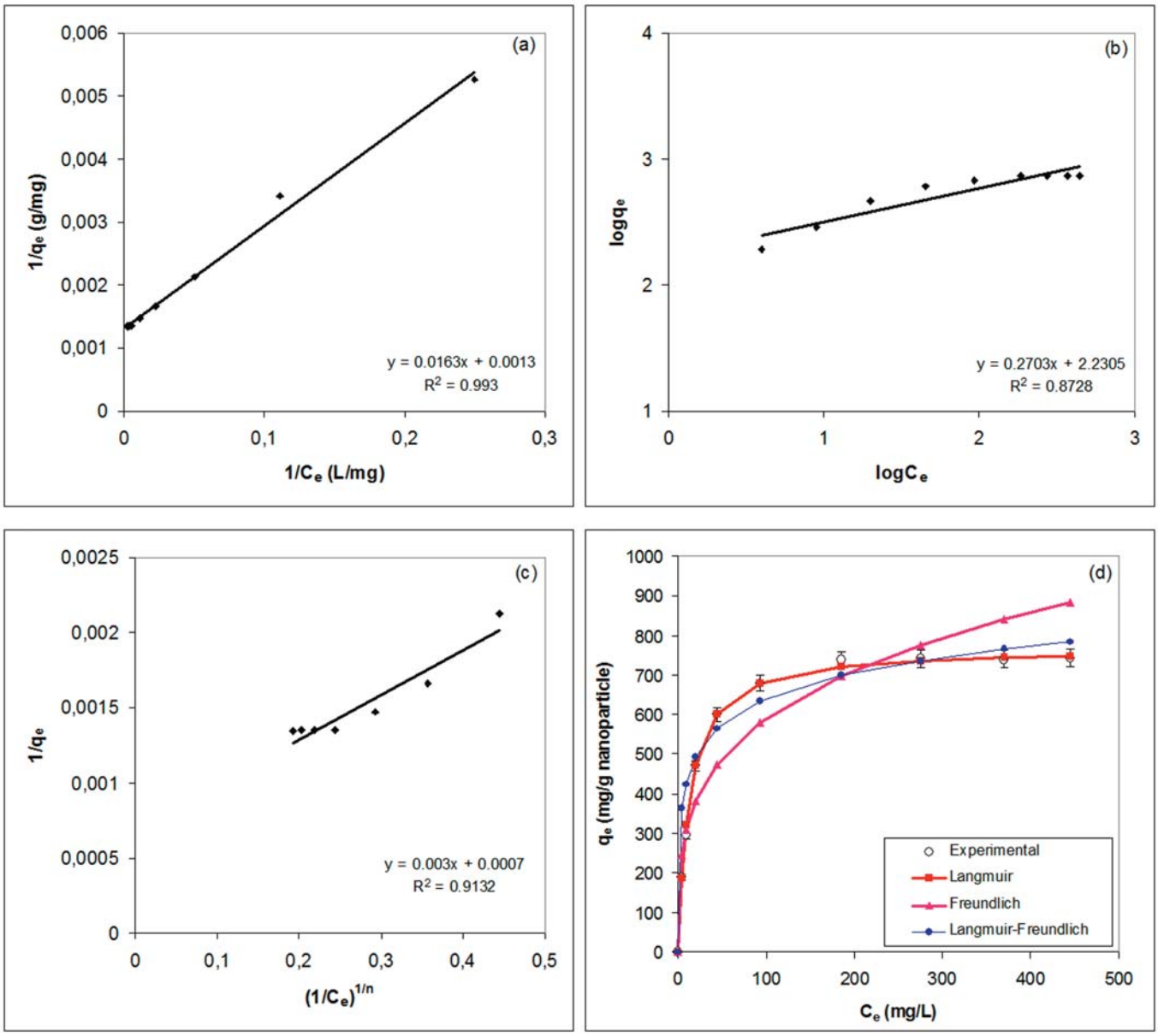

Figure 5. Adsorption isotherms. (a) Langmuir; (b) Freundlich; (c) Langmuir-Freundlich; (d) data fitted to the isotherm equations.

all theoretical approaches used in this study shows that the Langmuir equation fits the experimental data best.

It must be also noted that the standard deviation of the values determined by regression analysis is comparatively low. It must be also pointed out that the experimental adsorption capacities for PHEMA-IMEO nanoparticles are lower than to the theoretical adsorption capacities (i.e., obtained from adsorption models). This difference is due to the steric/geometric hindrances (i.e., accessibility) between the analyte ion (Hg^{2+}) and the binding sites (IMEO) on the surface of PHEMA nanoparticles.

Effect of pH

pH is the most critical parameter for metal adsorption as it influences both the polymer surface chemistry as well as the solution chemistry of soluble metal ions. Due to the deprotonation of the the metal complexing ligand (IMEO), its adsorption behavior for metal ions is influenced by the pH value, which affects the surface structure of adsorbent, the formation of metal hydroxides, and the interaction between adsorbent and metal ions. Therefore, in order to establish the effect of pH on the adsorption of Hg^{2+} onto the both the PHEMA and the PHEMA-IMEO nanoparticles, we repeated the batch adsorption equilibrium studies at different pHs

in the range of 2.0-7.0. In this group of experiments, the equilibrium concentration of Hg^{2+} and the adsorption equilibrium time were 43 mg/L and 2 h, respectively. The pH dependence of adsorption values of Hg^{2+} is shown in Figure 6. In the case of PHEMA nanoparticles, adsorption is pH independent. But, it is indicated that the adsorption of Hg^{2+} onto the PHEMA-IMEO nanoparticles was pH dependent. The results show that Hg^{2+} adsorption by the PHEMA-IMEO nanoparticles was very low at pH 2.0, but increased rapidly with increasing pH and then reached the maximum at pH 5.0. The competitive adsorption of hydrogen ions with Hg^{2+} ions for imidazole groups at lower pH values accounts for the observed low adsorption capacity. Since the imidazole groups are most likely protonated at a low pH, the nanoparticles are positively charged, resulting in a strong electrostatic repulsive forces between the IMEO on the nanoparticles and positively charged metal ions. Hg^{2+} adsorption around pH 3.0-4.0 was also low. It is well known in adsorption mechanisms, that a decrease in solubility favors an improvement in adsorption performance.

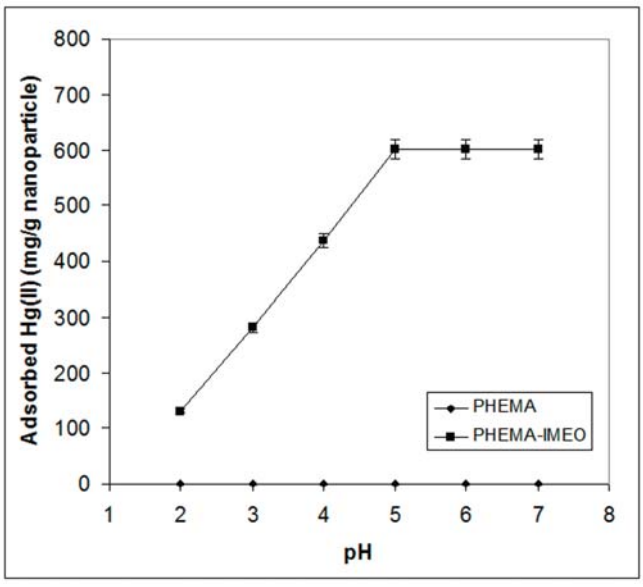

Figure 6. Effect of pH on adsorption of Hg^{2+} on the PHEMA and the PHEMA-IMEO nanoparticles: IMEO loading: 1021 μmol/g; Equilibrium concentration of Hg^{2+}: 43 mg/L.

Competitive Adsorption

As seen in Table 3, adsorbed amounts of Hg^{2+} ions are higher than those obtained for Cd^{2+} and Pb^{2+}, not only in weight basis but also in molar basis. The adsorption capacities are 238.8 mg/g for Hg^{2+}; 45.9 mg/g for Cd^{2+} and 19.6 mg/g for Pb^{2+}. From these results the order of affinity is $Hg^{2+} > Cd^{2+} > Pb^{2+}$. This trend is presented on the basis of mass (mg) metal adsorption per gram adsorbent and these units are important in quantifying respective metal capacities in real terms. However, a more effective approach, for this work is to compare metal adsorption on a molar basis; this gives a measure of the total number of metal ions adsorbed, as opposed to total weight, and is an indication of the total number of binding sites available on the adsorbent matrix, to each metal. Additionally the molar basis of measurement is the only accurate way of investigating competition in multi-component metal mixtures. Molar basis units are measured as μmol per gram of dry-adsorbent. It is evident from Table 3 that the order of capacity of PHEMA-IMEO nanoparticles is as follows: $Hg^{2+} > Cd^{2+} > Pb^{2+}$. It is clear from Table 3 that the PHEMA-IMEO nanoparticles showed more affinity to Hg^{2+} ions.

Table 3. Competitive adsorption of Hg^{2+}, Cd^{2+} and Pb^{2+} from their mixture onto PHEMA-IMEO nanoparticles: IMEO loading: 1021 μmol/g; pH: 5.0.

Metal ions	Metal ions adsorbed	
	(mg/g polymer)	(μmol/g polymer)
Hg^{2+}	238.8	1190.5
Cd^{2+}	45.9	408.3
Pb^{2+}	19.6	94.5

Behavior of the Elution

The regeneration of the adsorbent is likely to be a key factor in improving process economics. To be useful in metal remediation processes, metal ions should be easily eluted under suitable conditions. Elution of the Hg^{2+} from the metal-chelating nanoparticles was performed in a batch

experimental set-up. Various factors are probably involved in determining rates of Hg^{2+} elution, such as the extent of hydration of the metal ions and polymer microstructure. However, an important factor appears to be binding strength. When HNO_3 is used as the elution agent, the coordination spheres of chelated Hg^{2+} ions is disrupted and ubsequently Hg^{2+} ions are released from the nanoparticle surface into the desorption medium. In this study, the elution time was found to be 15 min. Elution ratios are very high (up to 99%). The ability to reuse the PHEMA-IMEO nanoparticles was shown in Figure 7. The adsorption behaviour is stable for ten cycles of use and it could be used at least 25 times. The adsorption capacity of the recyled nanoparticles can be maintained at 96% level at the 25th cycle. This means that the newly synthesized nanoparticles has great potential for industrial removal applications.

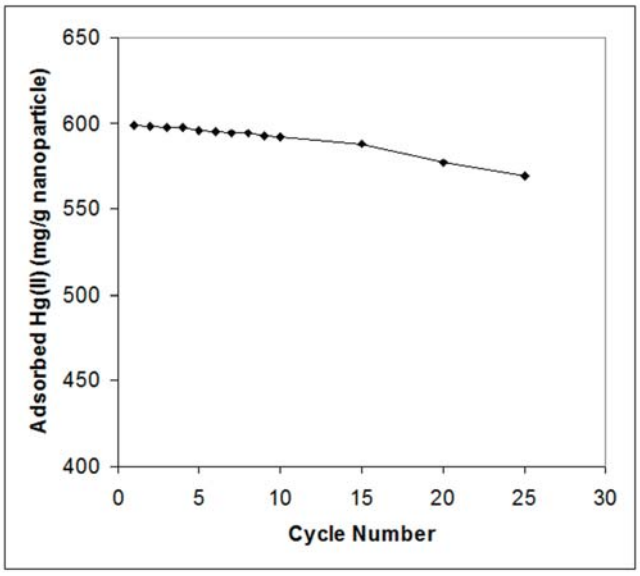

Figure 7. Adsorption-elution cycles for Hg^{2+}. Adsorption conditions; Hg^{2+} equilibrium concentration: 180 mg/L; pH: 5.0.

REFERENCES

1. Z.Y. Ma, Y.P. Guan, X.Q. Liu, H.Z. Liu, Langmuir, 21 (2005) 6987.
2. L. Sun, J. Dai, G.L. Baker, M.L. Bruening, Chem. Mater., 18 (2006) 4033.
3. J. Dai, Z. Bao, L. Sun, S.U. Hong, G.L. Baker, M.L. Bruening, Langmuir, 22 (2006) 4274.
4. K. Peng, K. Hidajat, M.S. Udin, J. Colloid Interf., Sci. 271 (2004) 277.
5. S.W. Choi, H.Y. Kwon, W.S. Kim, J.H. Kim, Colloids Surf A, 201 (2002) 283.
6. S. Lu, J. Ramos, J. Forcada, Langmur, 23 (2007) 12893.
7. X. Li, J.P. Hernandez, S.A. Haque, J.R. Durrant, E. Palomares, J. Mater. Chem., 17 (2007) 2028.
8. M. Takafuji, S. Ide, H. Ihara, Z. Xu, Chem. Mater., 16 (2004) 1977.
9. C. Lu, C. Liu, J. Chem. Technol. Biotechnol., 81 (2006) 1932.
10. L. Qi, Z. Xu, Colloids Surf A, 251 (2004) 183.
11. R. P. Singh, J. D. Way, S. F. Dec, J. Membr. Sci., 259 (2005) 34.
12. Z. Bilkova, M. Slovakova, D. Horak, J. Lenfeld, J. Churacek, J. Chromatogr. B, 770 (2002) 177.
13. N. Öztürk, M.E. Günay, S. AKgöl, A. Denizli, Biotehnol. Prog., 23 (2007) 1149.
14. M.F. Garcia, R.P. Garcia, N.B. Garcia, A. Sanz-Medel A. Talanta 1994, 41, 1833.
15. P.A. D'Itri, F.M. D'Itri, Mercury Contamination, Wiley, New York, 1977
16. E.P.C. Lai, B. Wong, V.A. Vandernoot, Talanta 1993, 40, 1097.
17. M. Berglund, B. Lind, K.A. Björnberg, B. Palm, O. Einarsson, M. Vahter, Environmental Health A 2005, 4, 20.
18. M. Aschner, J.L. Aschner, Am J Dis Child 1989, 143, 1133.
19. M.D. Martin, B.J. Williams, J.D. Charleston, D. Oda, Oral Surg 1997, 84, 495.
20. N. Öztürk, S. Akgöl, M. Arisoy, A. Denizli, A., Sep. Purif. Technol., 58 (2007) 83.
21. C.T. Lin, S.Y. Lee, E.S. Keh, D.R. Dong, H.M. Huang, Y.H. Shih, J. Oral. Rehabil., 27 (2000) 919.
22. C.J. Soares, M. Giannini, M.T. De Oliveira, L.A.M.S. Paulillo, L.R.M. Martins,

    J. Appl. Oral. Sci., 12 (2004) 1.
23. P. Silberzan, L. Leger, D. Ausserre, J.J. Benattar, Langmuir, 7 (1991) 1647.

24. M. Ahmaruzzaman, D.K. Sharma. J. Coll. Interf. Sci., 287 (2005) 14.

25. A. Lezzi, S. Cobianco and A. Roggrero, J. Polym. Sci Part A, 32 (1994) 1877.

26. A. Denizli, G. Özkan, J. Appl. Polym. Sci., 78 (2000) 81.

27. A. Denizli, K. Kesenci, E. Pişkin, React. Functl. Polym., 44 (2000) 235.

28. A. Jyo, S. Matsufune, H. Ono and H. Egawa, J Appl. Polym. Sci., 63 (1997) 1327.

29. B. Salih, R. Say, A. Denizli, O. Genc, E. Piskin, Anal. Chim. Acta, 371 (1998) 177.

30. S. Binman, S. Belfer, A. Shani, J Appl. Polym. Sci., 63 (1997) 625.

31. K. Kesenci, R. Say, A. Denizli, European Polym. J., 38 (2002) 1443.

32. D.C. Hwang and S. Damodaran, J. Appl. Polym. Sci., 64 (1997) 891.

33. A. Denizli, C. Arpa, S. Bektas, O. Genc, Adsorp. Sci. Technol., 20 (2002) 91.

34. C.Y. Liu, H.T. Chang and C.C. Hu, Inorg. Chim. Acta, 172 (1990) 151 .

35. S. Shah and S. Devi, React. Functl. Polym., 31 (1996) 1.

36. A.R. Cestari and C. Airoldi, J. Colloid Interf. Sci., 195 (1997) 338.

37. M.L. Delacour, E. Gailliez, M. Bacquet, M. Morcellet, J. Appl. Polym. Sci., 73 (1999) 899.

38. B.L. Rivas, H.A. Maturana, M.J. Molina, M.R. Gomez-Anton and I.F. Pierola, J. Appl. Polym. Sci., 67 (1998) 1109.

39. C. Arpa, A. Saglam, S. Bektas, S. Patır, O. Genc, A. Denizli, Adsorpt. Sci. Technol., 20 (2002) 203.

40. R.R. Navarro, K. Sumi, N. Fujii, M. Matsumara, Wat. Res., 30 (1996) 2488.

41. A. Denizli, S. Senel, G. Alsancak, N. Tuzmen, R. Say, React. Functl. Polym., 55 (2003) 121.

42. N.S.C. Becker and R.J. Eldridge, Reactive Polymers, 21 (1993) 5.

43. A. Denizli, B. Garipcan, S. Emir, S. Patir, R. Say, Adsorp. Sci. Technol., 20 (2002) 607.

44. R. Say, B. Garipcan, S. Emir, S. Patir, A. Denizli, Macromol. Mater. Eng., 287 (2002) 539.

45. R. Say, E. Birlik, Z. Erdemgil, A. Denizli, A. Ersöz, J. Hazardous Mater., 150 (2008) 560.

46. S. Senel, A. Kara, A. Karabakan, A. Denizli, J. Appl. Polym. Sci., 100 (2006) 1222.

47. H. Yavuz, A. Denizli, H. Gungunes, M. Safarikova, I. Safarik,, Sep. Purif. Technol., 52 (2006) 253.

48. A. Denizli, S. Senel, G. Alsancak, N. Tüzmen, R. Say, React. Functl. Polym., 55 (2003) 121.

49. A. Kara, L. Uzun, N. Besirli, A. Denizli, J. Hazardous Mater., 106 (2004) 93.

50. B. Garipcan, R. Say, A. Karbakan, S. Patir, A. Denizli, N-methacryloyl-L-glutamic acid incorporated poly(2-hydroxy ethyl methacrylate) beads for Hg^{2+} removal, in: Advances in Chemistry Research, Vol. 1, pp. 141-158, Nova Science Publishers, F.L. Gerard ed., 2006.